

MIT Open Access Articles

*PYRITIZED CRYOGENIAN CYANOBACTERIAL
FOSSILS FROM ARCTIC ALASKA*

The MIT Faculty has made this article openly available. *Please share* how this access benefits you. Your story matters.

Citation: Moore, Kelsey R. et al. "PYRITIZED CRYOGENIAN CYANOBACTERIAL FOSSILS FROM ARCTIC ALASKA." PALAIOS 32, 12 (December 2017): 769–778 © 2017 Society for Sedimentary Geology

As Published: <https://doi.org/10.2110/palo.2017.063>

Publisher: Society for Sedimentary Geology

Persistent URL: <http://hdl.handle.net/1721.1/120081>

Version: Author's final manuscript: final author's manuscript post peer review, without publisher's formatting or copy editing

Terms of use: Creative Commons Attribution-Noncommercial-Share Alike



1 **PYRITIZED CRYOGENIAN CYANOBACTERIAL FOSSILS FROM ARCTIC**
2 **ALASKA**

3 KELSEY R. MOORE,¹ TANJA BOSAK,¹ FRANCIS MACDONALD,² KIMBERLY
4 DU,³ SHARON A. NEWMAN,¹ DANIEL J. G. LAHR,⁴ SARA B. PRUSS^{3*}

5 ¹*Massachusetts Institute of Technology, Department of Earth, Atmospheric and Planetary*
6 *Sciences, Cambridge, Massachusetts 02139, USA*

7 ²*Harvard University, Department of Earth and Planetary Sciences, Cambridge,*
8 *Massachusetts 02138, USA*

9 ³*Department of Geosciences, Smith College, Northampton, Massachusetts 01063, USA*
10 *email: spruss@smith.edu*

11 ⁴*Department of Zoology, University of São Paulo, São Paulo SP 05508-90, Brazil*

12 *Corresponding author.

13 RRH: *FOSSILS FROM THE IKIAKPUK FORMATION*

14 LRH: *MOORE ET AL.*

15 Keywords: Cyanobacteria, Snowball Earth, *Obruchevella*, pyritization

16
17 **ABSTRACT**

18
19 **The Cryogenian was a time of climatic extremes, with two extended and**
20 **severe global glaciations bracketing hothouse conditions. The effect of these extreme**
21 **climate conditions on ocean chemistry and the marine biosphere remain poorly**
22 **understood. Most of the previous studies of the fossil record from this interval focus**
23 **on benthic organisms, with few examples of organisms with an inferred planktonic**

24 **lifestyle and no firm evidence for photosynthetic organisms. Here, we present**
25 **helically coiled, straight, and curved fossils composed of fine crystalline or**
26 **framboidal pyrite in limestone samples from the Ikiakpuk formation of Arctic**
27 **Alaska. These structures are morphologically identical to fossils of *Obruchevella*, a**
28 **cyanobacterial form genus that has been reported in pre-Sturtian and post-**
29 **Marinoan strata, but not in deposits from the Cryogenian non-glacial interlude. We**
30 **interpret fossils of the Ikiakpuk formation as planktonic cyanobacteria based on**
31 **their morphology, which is identical to that of some modern planktonic**
32 **cyanobacteria. Further evidence for a planktonic lifestyle comes from the**
33 **preservation of these pyritized fossils in deep-water facies that lack evidence of**
34 **microbial lamination. They provide the first direct evidence for bacterial primary**
35 **productivity in the pelagic realm during the Cryogenian non-glacial interlude.**

36

37

INTRODUCTION

38

39 The Earth experienced two Neoproterozoic Snowball Earth events: the older
40 Sturtian (~717-660 Ma) and the younger Marinoan (>640-635 Ma) glaciations (Rooney
41 *et al.*, 2015). During the Sturtian glaciation, glaciers are thought to have been ~1000 m
42 thick on the continents (Liu and Peltier, 2010) and oceans (Tziperman *et al.*, 2012), with
43 ice extending to the equator. The low temperature and ice covering the oceans decreased
44 the availability of liquid water and sunlight, and likely reduced primary productivity
45 (Costas *et al.*, 2008). As a result of the stress placed on microbial ecosystems during the
46 Sturtian glaciation, it has been suggested that there was a significant decrease in diversity

47 during the 20 million years of the Cryogenian non-glacial interlude (Riedman et al.,
48 2014; Cohen and Macdonald, 2015). The interval during and after the deglaciation saw
49 greenhouse conditions with increased temperatures and other rapid changes in pCO₂,
50 continental weathering, alkalinity, and salinity (Hoffman et al., 1998; Kasemann et al.,
51 2005; Bao et al., 2008), though many of these environmental conditions were likely short
52 lived. The effects of these changes on the emerging biosphere are poorly constrained,
53 largely due to the scarcity of fossil assemblages described from this time.

54 Sedimentary deposits that sample a range of environments and lithologies enable
55 the assessment of biodiversity during the Cryogenian non-glacial interlude. Most
56 recently, this has included investigation of cap carbonates deposited after the Sturtian
57 glaciation. For example, fossil assemblages in the dark, micritic facies of cap carbonates
58 in Zambia, Namibia, and Mongolia preserve communities of diverse eukaryotes (Bosak
59 et al., 2011a; Dalton et al., 2013; Moore et al., 2017). These communities include a
60 variety of agglutinated testate eukaryotes (Bosak et al., 2011a, 2012; Dalton et al., 2013;
61 Moore et al., 2017), some organic-walled fossils of presumed planktonic eukaryotes from
62 cap carbonates (Bosak et al., 2011b), benthic eukaryotes from later Cryogenian
63 carbonates (Cohen et al., 2015), and organic remnants of filamentous and coccoidal
64 microorganisms (Bosak et al., 2011a). In contrast, analyses of the siliciclastic facies
65 including glacial deposits and shales deposited after the Sturtian glaciation reveal rare
66 spheroidal vesicles, interpreted as eukaryotes, and few examples of filamentous
67 microfossils, interpreted broadly as the remnants of bacteria (Riedman et al., 2014).
68 However, the simple morphologies of these fossils prevent further characterization of
69 their taxonomic identity, and hinder inferences relating to the life modes of such

70 organisms before death and burial (Riedman et al., 2014). The abundance and
71 morphological diversity of fossils found in carbonates from the Cryogenian non-glacial
72 interlude, therefore, highlight the importance of continued investigation of carbonate
73 facies to build a more complete fossil record from this interval.

74 Here, we describe an assemblage of pyritized microfossils that were preserved in
75 Cryogenian limestone of the Ikiakpuk formation in Arctic Alaska (Strauss et al., in press).
76 Such microfossils have never before been described from this interval and come from
77 strata that are distally deposited age equivalents of Cryogenian platform carbonates of
78 unit 1 of the Katakaturuk Dolomite (Macdonald et al., 2009). The limestone samples
79 contain pyritized fossils with distinct coiled morphologies that are identical to the
80 previously described fossil *Obruchevella*, interpreted as a fossil of a type of
81 photosynthetic cyanobacterium analogous to some modern planktonic cyanobacteria.
82 This finding provides the first direct evidence of oxygenic, photosynthetic bacteria that
83 were primary producers in the marine water column during the Cryogenian non-glacial
84 interlude.

85

86 GEOLOGIC SETTING

87

88 Fossils were recovered from thin-bedded black limestone of the informal
89 Ikiakpuk formation (Strauss et al., accepted), sampled in the Fourth Range of Arctic
90 Alaska (Figure 1). This unit has previously been referred to as the “Black Limestone” or
91 “Fourth Range Limestone” (Macdonald et al., 2009 and references therein). Carbon and
92 strontium isotope chemostratigraphy suggest that the Ikiakpuk formation is Cryogenian in

93 age and a deep-water equivalent of unit K1 of the Katakturuk Dolomite in the
94 Sadelerochit, Shublik, and Kikiktat Mountains (Macdonald et al., 2009; Strauss et al., in
95 press). Unit K1 consists predominantly of shallow marine dolostone and contains a
96 Sturtian-age cap carbonate that overlies the Hula Hula diamictite. A maximum age on the
97 Hula Hula diamictite is provided by a U/Pb zircon date of 719.47 ± 0.29 Ma on the
98 underlying Kikiktat volcanics (Cox et al., 2015). Globally, strata deposited in the
99 Cryogenian non-glacial interlude are constrained in age between ca. 660 Ma and >635
100 Ma (Rooney et al., 2015).

101 In the Fourth Range, the Ikiakpuk formation is ~1000 m thick and consists
102 predominantly of thin-bedded, platy limestone with minor shale and sandstone
103 (Macdonald et al., 2009). The base of the Ikiakpuk formation is not exposed and is
104 unconformably overlain by the Devonian-Carboniferous Endicott and Lisburne groups.
105 The samples analyzed here come from 10.3 to 49 m of the Ikiakpuk formation in the
106 Fourth Range. The limestone lacks microbial lamination and some samples display
107 normal grading from calcisiltite to micrite, consistent with lower-slope turbidite
108 deposition on the flanks of a carbonate bank (Macdonald et al., 2009; Strauss et al., in
109 press). Dark micritic limestone facies were sampled for this study because previous work
110 on carbonates from the Cryogenian non-glacial interlude have shown that they are more
111 likely to preserve fossils than lighter, more cement-rich facies or other carbonate facies
112 (e.g. Bosak et al., 2011a; supplemental material in Bosak et al., 2012; Dalton et al.,
113 2013). Future work will focus on examining different facies.

114

115

METHODS

116

117 Twelve samples from dark, unlaminated limestone facies of the Ikiakpuk
118 formation that covered ~40 m of section were analyzed in this study. Approximately 4-10
119 g of each sample was placed in a solution of 10% HCl to remove any surficial
120 contaminants, and was then dissolved in a solution of 10% acetic acid buffered with 0.65
121 M hydrated ammonium acetate to produce a residue containing microfossils following
122 Dalton et al. (2013). The residues were filtered through 0.2 μm , 41 μm , and 100 μm
123 Millipore nylon net filters (EMD Millipore, HNWP04700, NY4104700, and
124 NY1H04700, Billerica, MA, USA) using vacuum filtration. A Nikon SMZ645
125 stereoscopic microscope was used to examine residues in the >100 μm and the 41-100
126 μm size fractions, because those sizes were previously shown to contain microfossils
127 (e.g., Dalton et al., 2013). Structures that had repeating morphologies and were distinct
128 from the angular minerals in the surrounding residues were isolated for further analysis.
129 Such structures occurred in eight of the twelve samples.

130 Samples with distinct morphological characteristics were imaged using a scanning
131 electron microscope (FEI Quanta 450, Smith College, Northampton, MA). Before
132 imaging, samples were placed on 12.7 mm diameter SEM stubs (Ted Pella Inc., Product
133 #16111, Redding, CA, USA) with 12 mm ultra thin carbon adhesive tabs (Electron
134 Microscopy Sciences, Product #77825-12-SP, Hatfield, PA) and coated with gold and
135 palladium using a Hummer V Sputter Coater (Smith College, Northampton, MA). We
136 used EDS Team software with the 20 kV acceleration voltage to analyze the elemental
137 composition of structures using point analyses and elemental mapping.

138 To determine whether organic carbon was present in putative microfossils, we
139 acquired their Raman spectra using a Horiba LabRam Evolution Spectrometer (Harvard
140 University, Center for Nanoscale Systems, Cambridge, MA) at 50X magnification.
141 Samples were placed on glass slides and spectra were collected at 50X magnification
142 using a 633 nm wavelength laser. Data were analyzed with LabSpec software. We also
143 examined thin sections of the eight samples determined to be fossiliferous by residue
144 analysis to further characterize the mineralogy of the limestone matrix and the fossils, but
145 microfossils observed in thin section were generally rare.

146

147 RESULTS

148

149 Morphology

150

151 Residues from the Ikiakpuk formation contained microfossils with coiled
152 morphologies that were not previously reported at other fossiliferous localities from this
153 time. A total of 44 microfossils were identified in 8 out of 12 analyzed samples. The
154 structures included both coil fragments and complete coils that exhibited varying degrees
155 of degradation (Figure 2). Coiled structures consisted of a single solid strand, ~20 μm to
156 30 μm -thick, wound helically into a coil. Coil diameters ranged from ~50 μm to 170 μm .
157 Some specimens had a uniform grainy, fine crystalline texture (18 out of 44 specimens;
158 e.g., Figure 2.A), while others had ~5 μm to 10 μm -wide spherical structures embedded
159 within the strands (26 out of 44 specimens; e.g. sample 3.A). The textures and
160 thicknesses of the strands were consistent among specimens and across samples from

161 different parts of the examined ~40 m of limestone. In most specimens, the strand was
162 wound tightly into a helically coiled, hollow cylinder ~50 μm to 170 μm in diameter
163 (Figure 2.A, B, C, D). Some forms were more loosely coiled (Figure 2.E, F), and many
164 fragments of coiled structures were present as curved (Figure 3.A, B) or straight strands
165 (Figure 3.C, D) between ~70 μm and 200 μm -long and ~20 μm to 40 μm -wide. The
166 loosely coiled structures were still broadly helical and appeared to have been either
167 compressed or uncoiled.

168

169 Chemical Data and Petrography

170

171 To understand the processes that preserved microfossils in the Ikiakpuk
172 formation, we determined the elemental composition of microfossils using Energy
173 Dispersive X-ray Spectra (EDS) spectra and chemical maps. These showed strong iron
174 and sulfur peaks (Figure 4) consistent with the mineral pyrite (FeS_2) in specimens from
175 all samples. Pyrite was also present as cubes and framboids in the insoluble residues. We
176 used additional chemical analysis with Raman spectroscopy to determine whether or not
177 the process of pyritization preserved organic matter in the microfossils. Spectra revealed
178 that microfossils contained carbonaceous material, shown by distinct peaks at ~1348 cm^{-1}
179 and ~1609 cm^{-1} (Figure 5), consistent with a D-band and G-band Raman shift indicative
180 of organic carbon (e.g., Ferrari and Robertson, 2000; McNeil et al., 2015).

181 We examined petrographic thin sections of limestone samples that yielded fossils
182 in the preceding residue analysis to demonstrate that microfossils were found *in situ*.
183 Microfossils were difficult to identify in thin sections of limestone samples from the

184 Ikiakpuk formation, perhaps because both the microfossils and the microcrystalline
185 limestone matrix were dark, or because fossils were generally rare. However, we
186 identified a few distinct examples in thin section, with cross sections of the coiled helices
187 visible as two parallel lines of dark circles separated by $\sim 50 \mu\text{m}$ of micrite (Figure 6).
188 These dark circles were mineralogically distinct, as demonstrated by their dark, opaque
189 appearance against the surrounding micritic matrix and demonstrated that the
190 microfossils were preserved *in situ*.

191

192

DISCUSSION

193

194

Interpretation of pyritized structures

195

196

197

198

199

200

201

202

203

204

205

206

Coiled structures of the Ikiakpuk formation of Arctic Alaska closely resemble the previously described fossil *Obruchevella* (Knoll and Ohta, 1988; Knoll, 1992; Mankiewicz, 1992; Butterfield and Rainbird, 1998). The oldest *Obruchevella* were found in shales of the Neoproterozoic Wynniatt Formation of arctic Canada ($\sim 800 \text{ Ma}$; Butterfield and Rainbird, 1998), in which the three dimensional, organic-walled, coiled fossils had an overall helix diameter of $\sim 40 \mu\text{m}$ and were made up of filaments $\sim 10 \mu\text{m}$ -wide. These fossils are one component of a more diverse fossil assemblage that includes other filamentous morphologies as well as acritarchs (Butterfield and Rainbird, 1998). *Obruchevella* have also been identified as a component of assemblages containing other organic-walled filaments in younger siliciclastic deposits that postdate the Marinoan glaciation. Fossils preserved in chert in metasedimentary rocks of the Neoproterozoic

207 Baklia Formation from the Prins Karls Forland, western Svalbard, (Ediacaran in age) are
208 morphologically similar to those of the Wynniatt Formation, comprised of single
209 filaments helically coiled into cylinders (Knoll and Ohta, 1988; Knoll, 1992). The
210 Ediacaran fossils are described in two size classes: a smaller form with strand diameters
211 $\sim 4 \mu\text{m}$ to $5 \mu\text{m}$ and cylindrical coil diameters between 25 and $30 \mu\text{m}$, and a larger form
212 with strand diameters $\sim 28 \mu\text{m}$ to $33 \mu\text{m}$ and cylindrical coil diameters up to $230 \mu\text{m}$
213 (Knoll and Ohta, 1988; Knoll, 1992). Mankiewicz (1992) also described *Obruchevella*
214 from the Burgess Shale (middle Cambrian), and these have variable helix ($36.4 \mu\text{m}$ to
215 $71.5 \mu\text{m}$) and filament diameters ($9.1 \mu\text{m}$ to $18.2 \mu\text{m}$). The largest fossils of the
216 Cambrian assemblages have coil and filament diameters similar to the largest
217 *Obruchevella* from the Prins Karls Forland (Knoll and Ohta, 1988; Knoll, 1992), and
218 both are nearly identical in size and shape to those of the Ikiakpuk formation.

219 Other occurrences include 2-3 μm -wide, helically coiled *Obruchevella* from the
220 pre-Sturtian Chichkan Formation of Kazakhstan preserved in chert (~ 800 to 750 Ma ;
221 Sergeev and Schopf, 2010) and $\sim 40 \mu\text{m}$ -wide loosely coiled *Obruchevella* in chert
222 nodules from the post-Marinoan Doushantuo Formation of China (~ 600 - 550 Ma ; Zhang
223 et al., 1998; Xiao, 2004). Both of these occurrences have identical shapes to coiled
224 microfossils preserved in the Ikiakpuk formation. The previously described occurrences
225 of *Obruchevella* span $\sim 300 \text{ My}$ period between their first appearance Neoproterozoic
226 ($\sim 800 \text{ Ma}$) and those preserved in the middle Cambrian Burgess Shale ($>500 \text{ Ma}$).
227 However, there has been a clear gap in the fossil record of *Obruchevella* between the
228 beginning of the Sturtian glaciation and end of the Marinoan glaciation. The fossils
229 described here are morphologically identical to previously described *Obruchevella*, and

230 are the first occurrence of these fossils to bridge that gap. Their presence in limestone
231 deposited during the Cryogenian non-glacial interlude shows that these cyanobacteria not
232 only survived in geographically restricted environments through the glaciations, but were
233 also an important component as primary producing organisms in some pelagic marine
234 ecosystems during or after the deglaciation.

235 The coiled structures of the Ikiakpuk formation are analogous to the range of
236 morphologies described in previous assemblages of *Obruchevella*, with tightly coiled
237 helices identical to those of the Baklia, Wynniatt and Chichkan formations (Knoll and
238 Ohta, 1988; Knoll, 1992; Butterfield and Rainbird, 1998), and loosely coiled forms
239 similar to those of the Doushantuo Formation (Zhang et al., 1998; Xiao, 2004).

240 Furthermore, coils of the Ikiakpuk formation have size ranges (strand diameters ~20 µm
241 to 30 µm and total structure diameter ~50 µm to 170 µm) comparable to the larger classes
242 of *Obruchevella* described in the Baklia Formation (Knoll and Ohta, 1988), the Wynniatt
243 Formation (Butterfield and Rainbird, 1998), and the Burgess Shale (Mankiewicz, 1992).
244 The straight and curved strands of the Ikiakpuk formation are less diagnostic than the
245 coiled structures, and may be either fragments of *Obruchevella* or remnants of other
246 filamentous bacteria with uncertain taxonomic affinities.

247 The microfossils described here as well as some previously described
248 *Obruchevella* fossils are much larger than most modern cyanobacteria, but their helically
249 coiled morphology closely resembles that of modern cyanobacteria including *Spirulina*,
250 *Cyanospira*, *Arthrospira*, and some species of *Anabaena* (Florenzano et al., 1985;
251 Margheri et al., 2003; Komárek and Zapomělová, 2007). All of these modern groups
252 have helically coiled trichomes that can be either loosely coiled (e.g., *Cyanospira* and

253 *Anabaena*; Florenzano et al., 1985; Komárek and Zapomělová, 2007) or tightly coiled
254 (e.g., *Spirulina*; Margheri et al., 2003). In fact, some species such as *Cyanospira*
255 *capsulata* possess a mucilaginous capsule that creates a single smooth coating over the
256 trichome with diameters up to ~20 µm (Sili et al., 2011), consistent with the size of coiled
257 structures of the Ikiakpuk formation (Figure 2).

258 Some modern filamentous algae, such as *Spirogyra*, *Zygnema*, *Mougeotia*, and
259 *Klebsormidium*, have cell diameters of >10 µm (Pouličková et al., 2007; Mikhailyuk et
260 al., 2014), but these lack the coiled morphology characteristic of the microfossils
261 described here. In the case of *Spirogyra*, it is the chloroplast organelle that demonstrates a
262 spiraled morphology, not the filamentous organism itself, and the chloroplast has a width
263 of <10 µm (Wongsawad and Peerapornpisal, 2015), much smaller than the fossils of the
264 Ikiakpuk Formation. Filamentous sulfur oxidizing bacteria like *Beggiatoa* have similar
265 cell widths up to 200 µm, but lack any spiraled morphology (Salman et al., 2013). Some
266 strains of sulfate reducing bacteria have been described as spiraled, including some
267 species of *Desulfovibrio* and *Desulfonatronospira* (Caumette et al., 1991; Tee et al.,
268 1996; Castro et al., 2000; Sorokin and Chernyh, 2017), but these forms are rod shaped,
269 occasionally forming wavy chains (e.g., Zaarur et al., 2017). Such morphological
270 characters are entirely distinct from the long, wide, tightly coiled filaments of the
271 Ikiakpuk formation.

272 In summary, two arguments can be made in support of a cyanobacterial origin for
273 the pyritized coiled fossils described here: 1) fossils of the Ikiakpuk formation are
274 morphologically identical to the larger size classes of previously described *Obruchevella*,
275 which have been interpreted as cyanobacteria (Knoll and Ohta, 1988; Knoll, 1992;

276 Mankiewicz, 1992; Butterfield and Rainbird, 1998), and 2) these and previously
277 described *Obruchevella* are similar to modern coiled planktonic cyanobacteria
278 (Florenzano et al., 1985; Tomaselli, 1997; Tomaselli et al., 1997; Margheri et al., 2003;
279 Komárek and Zapomělová, 2007)—whose morphologies are not found among other
280 modern bacterial or eukaryotic groups.

281

282 Preservation and Depositional Environment

283

284 All microfossils described here are composed of pyrite (FeS₂; Figure 5), and
285 pyrite is also present in the insoluble residues as grains. Pyritization is an important form
286 of fossil preservation in both Proterozoic and Phanerozoic fossil assemblages (e.g.,
287 Oehler and Logan, 1977; Steiner and Reitner, 2001; Anderson et al., 2011; Wacey et al.,
288 2013; Borjigin et al., 2014). The pyrite framboids and the smooth, fine-crystalline pyrite
289 that preserves fossils in the Ikiakpuk formation (Figures 2 and 3) closely resemble
290 pyritized filamentous fossils reported in the Proterozoic McArthur H.Y.C. deposit
291 (Oehler and Logan, 1977), the Neoproterozoic Ust-Pinega Formation of Russia (Steiner
292 and Reitner, 2001) and the Ediacaran Doushantuo Formation of China (Anderson et al.,
293 2011; Borjigin et al., 2014). Still, few examples of pyritized filamentous fossils
294 interpreted as bacteria have been reported in Proterozoic sediments, and those that are
295 known are preserved in siliciclastic deposits from either before the Sturtian glaciation or
296 after the Marinoan glaciation. The fossils from the Ikiakpuk formation are the first
297 examples of preservation by pyritization in carbonates of the Cryogenian non-glacial
298 interlude, and are one of the few examples of pyritized bacteria in the fossil record.

299 This study is among one of the few three-dimensional analyses of *Obruchevella*,
300 which is largely possible due to their unique preservation by pyrite within carbonate
301 rocks. Previously described assemblages of *Obruchevella* are preserved as organic
302 remnants compressed in shales and cherts, and are therefore predominantly studied
303 petrographically, although Butterfield and Rainbird (1998) were also able to isolate three-
304 dimensional organic-walled fossils using HF dissolution in addition to their petrographic
305 analyses. The preservation of *Obruchevella* in dark, unlaminated limestone is unique for
306 this interval and rare for these fossils, and highlights an important distinction between the
307 environment in which these organisms lived and the environment in which they were
308 preserved. *Obruchevella* are the remnants pelagic photosynthetic bacteria that lived in
309 surface waters, but were preserved by pyritization in deep-water carbonates that lack
310 microbial lamination. Raman spectra reveal the presence of the D- and G-bands of fossil
311 kerogen (Figure 5), which further support an originally carbonaceous composition of the
312 structures and suggest that pyrite precipitated immediately around and within the
313 formerly organic filaments, which preserved the shape of the filaments. The preservation
314 of these organic filaments by pyrite and the occurrence of pyrite in the insoluble residues
315 not associated with the fossils suggests that the zone of sulfate reduction and sulfide
316 release was very close to the sediment-water interface, possibly extending up into the
317 water column. The organisms would have sunk to the seafloor after death, where they
318 were preserved through localized and rapid post-mortem pyritization prior to degradation
319 in the carbonate sediments.

320

321

Microbial Ecology

322

323 Microfossils preserved in the Ikiakpuk formation contribute to our growing
324 understanding of the marine realm during the Cryogenian non-glacial interlude, and
325 suggest a clear presence of primary productivity in the pelagic marine realm during this
326 greenhouse interval. The coiled structures and fragments are identical to previously
327 described *Obruchevella*, interpreted as photosynthetic cyanobacteria (Knoll and Ohta,
328 1988; Knoll, 1992; Mankiewicz, 1992; Butterfield and Rainbird, 1998). The life mode of
329 *Obruchevella* preserved in the Ikiakpuk formation is different from that of agglutinated or
330 carbonaceous benthic eukaryotes preserved in the Rasthof Formation of Namibia, the
331 Kakontwe Formation of Zambia, and the Taishir Formation of Mongolia (Bosak et al.,
332 2011a, 2012; Dalton et al., 2013; Cohen et al., 2015; Moore et al., 2017), which are
333 interpreted as eukaryotic organisms similar to testate amoebae, foraminifera, or other
334 unicellular eukaryotes or multicellular algae. Riedman *et al.* (2014) identified filamentous
335 *Siphonophycus* sp. and *Rugosoopsis tenuis* in shale deposits from the Cryogenian non-
336 glacial interlude, though the ecological niche of these organisms was not specified, and
337 other occurrences of *Siphonophycus* have been reported in benthic rather than planktonic
338 assemblages (Buick and Knoll, 1999). The fossils described here—identical to some
339 older and younger *Obruchevella*, which were previously interpreted as cyanobacteria
340 (Knoll and Ohta, 1988; Knoll, 1992; Mankiewicz, 1992; Butterfield and Rainbird,
341 1998)—provide the first direct evidence that planktonic, photosynthetic, oxygen-
342 producing organisms were present in surface waters during this interval.

343 Little is known about the recovery of the biosphere following the Sturtian
344 glaciation. The few fossil assemblages preserved in marine deposits from the Cryogenian

345 non-glacial interlude are key to understanding the response of organisms and ecosystems
346 to the hypothesized environmental conditions during this time. This is especially true for
347 fossils from the Ikiakpuk formation. *Obruchevella* first appear in the fossil record during
348 the Neoproterozoic, and were described in formations that both predate and postdate the
349 Snowball Earth events. Therefore, it follows that these organisms must have survived
350 through these events. However, to the best of our knowledge, this study provides the first
351 tangible evidence for the presence of such organisms in post-Sturtian marine ecosystems.
352 The morphology of *Obruchevella* is interpreted as diagnostically cyanobacterial, as has
353 been previously suggested (Knoll and Ohta, 1988; Knoll, 1992; Mankiewicz, 1992;
354 Butterfield and Rainbird, 1998). The presence of cyanobacteria in the Ikiakpuk formation
355 suggests that these organisms were the main primary producers in surface waters, and
356 that the overall morphological and species diversity was limited. However, further studies
357 of carbonate deposits from the Cryogenian non-glacial interlude are necessary to test the
358 hypothesis of limited diversity against the alternative hypothesis of taphonomic bias.

359

360

CONCLUSIONS

361

362 The Ikiakpuk formation of Arctic Alaska preserves fossils of photosynthetic,
363 planktonic organisms that lived during the Cryogenian non-glacial interlude. We interpret
364 fossils recovered in this study with distinctly coiled morphologies as *Obruchevella*
365 because their coiled morphology is identical to that of previously described older and
366 younger fossil occurrences of *Obruchevella* and to some modern planktonic
367 cyanobacteria such as *Spirulina*, *Cyanospira*, or *Anabaena*. Microfossils are preserved as

368 pyritized internal molds, indicating that pyrite formed inside of the cells soon after the
369 organisms died. In contrast to previously studied carbonates from this interval—including
370 the Kakontwe, Taishir and Rasthof formations, which preserve agglutinated and other
371 benthic eukaryotic organisms—the Ikiakpuk formation was deposited in a deeper water
372 setting and preserved mostly planktonic cyanobacteria. The fossil cyanobacteria
373 preserved in the Ikiakpuk formation provide the first direct evidence of photosynthetic,
374 oxygen-producing, planktonic organisms in the marine realm following the Sturtian
375 glaciation, and expand our understanding of the pelagic ecosystem and the preservational
376 conditions of deep-water settings during the Cryogenian non-glacial interlude. The
377 presence of coiled and straight filaments, and the absence of other morphologies in this
378 assemblage may indicate a reduced diversity in open marine ecosystems during this
379 interval, though further time-equivalent marine deposits are necessary to fully address
380 this hypothesis.

381

ACKNOWLEDGMENTS

382

383

384 We thank the Smith College Tomlinson Fund, the Smith College Geosciences
385 Department, the MIT NAI node, and a grant from the Simons Foundation ([344707],
386 [TB]) for funding this research. We thank Andrew Knoll for helpful conversations and
387 assistance with fossil identification and Justin Strauss for helping with stratigraphic
388 context. We also thank J. Wopereis, J. Brady, M. Vollinger, and A. McClelland for
389 assistance with sample analyses, M. Abedinejad and D. Kortes for technical support, and
390 the Bosak and Pruss labs for their support and conversations.

391

392

REFERENCES

393

394 ANDERSON, E.P., SCHIFFBAUER, J.D., AND XIAO, S., 2011, Taphonomic study of Ediacaran
395 organic-walled fossils confirms the importance of clay minerals and pyrite in
396 Burgess Shale-type preservation: *Geology*, v. 39, p. 643–646, doi:
397 10.1130/G31969.1.

398 BAO, H., LYONS, J.R., AND ZHOU, C., 2008, Triple oxygen isotope evidence for elevated
399 CO₂ levels after a Neoproterozoic glaciation: *Nature*, v. 453, p. 504–506, doi:
400 10.1038/nature06959.

401 BORJIGIN, T., YIN, L., BIAN, L., YUAN, X., ZHOU, C., MENG, F., XIE, X., AND BAO, F., 2014,
402 Nano-scale spheroids and fossils from the Ediacaran Doushantuo Formation in
403 China: *The Open Paleontology Journal*, v. 5, p. 1–9, doi:
404 10.2174/1874425701405010001.

405 BOSAK, T., LAHR, D.J.G., PRUSS, S.B., MACDONALD, F.A., DALTON, L., AND MATYS, E.,
406 2011a, Agglutinated tests in post-Sturtian cap carbonates of Namibia and
407 Mongolia: *Earth and Planetary Science Letters*, v. 308, p. 29–40, doi:
408 10.1016/j.epsl.2011.05.030. <http://dx.doi.org/10.1016/j.epsl.2011.05.030>.

409 BOSAK, T., LAHR, D.J.G., PRUSS, S.B., MACDONALD, F.A., GOODAY, A.J., DALTON, L.,
410 AND MATYS, E.D., 2012, Possible early foraminiferans in post-Sturtian (716–635
411 Ma) cap carbonates: *Geology*, v. 40, p. 67–70, doi: 10.1130/G32535.1.

412 BOSAK, T., MACDONALD, F., LAHR, D., AND MATYS, E., 2011b, Putative Cryogenian
413 ciliates from Mongolia: *Geology*, v. 39, p. 1123–1126, doi: 10.1130/G32384.1.

414 BUICK, R., AND KNOLL, A.H., 1999, Acritarchs and microfossils from the Mesoproterozoic
415 Bangemall Group, northwestern Australia: *Journal of Paleontology*, v. 73, p. 744–
416 764, doi: 10.1017/S0022336000040634.

417 BUTTERFIELD, N.J., AND RAINBIRD, R.H., 1998, Diverse organic-walled fossils, including
418 “possible dinoflagellates,” from the early Neoproterozoic of arctic Canada:
419 *Geology*, v. 26, p. 963–966, doi: 10.1130/0091-
420 7613(1998)026<0963:DOWFIP>2.3.CO;2.

421 CASTRO, H.F., WILLIAMS, N.H., AND OGRAM, A., 2000, Phylogeny of sulfate-reducing
422 bacteria: *FEMS Microbiology Ecology*, v. 31, p. 1–9, doi: 10.1111/j.1574-
423 6941.2000.tb00665.x.

424 CAUMETTE, P., COHEN, Y., AND MATHERON, R., 1991, Isolation and characterization of
425 *Desulfovibrio halophilus* sp. nov., a halophilic sulfate-reducing bacterium isolated
426 from Solar Lake (Sinai): *Systematic and Applied Microbiology*, v. 14, p. 33–38,
427 doi: 10.1016/S0723-2020(11)80358-9. <http://dx.doi.org/10.1016/S0723->
428 2020(11)80358-9.

429 COHEN, P.A., AND MACDONALD, F.A., 2015, The Proterozoic record of eukaryotes:
430 *Paleobiology*, v. 41, p. 610-632, doi: 10.1017/pab.2015.25.
431 http://www.journals.cambridge.org/abstract_S0094837315000251.

432 COHEN, P.A., MACDONALD, F.A., PRUSS, S., MATYS, E., AND BOSAK, T., 2015, Fossils of
433 putative marine algae from the Cryogenian glacial interlude of Mongolia: *Palaios*,
434 v. 30, p. 238–247, doi: 10.2110/palo.2014.069.
435 <http://palaios.sepmonline.org/cgi/doi/10.2110/palo.2014.069>.

436 COSTAS, E., FLORES-MOYA, A., AND LÓPEZ-RODAS, V., 2008, Rapid adaptation of
437 phytoplankters to geothermal waters is achieved by single mutations: were
438 extreme environments “Noah’s Arks” for photosynthesizers during the
439 Neoproterozoic “snowball Earth”? *New Phytologist*, v. 180, p. 922–932, doi:
440 10.1111/j.1469-8137.2008.02620.x.

441 COX, G.M., STRAUSS, J. V., HALVERSON, G.P., SCHMITZ, M.D., MCCLELLAND, W.C.,
442 STEVENSON, R.S., AND MACDONALD, F.A., 2015, Kikiktat volcanics of Arctic
443 Alaska – Melting of harzburgitic mantle associated with the Franklin large
444 igneous province: *Lithosphere*, v. 7, p. 275–295, doi: 10.1130/L435.1.
445 <http://lithosphere.gsapubs.org/cgi/doi/10.1130/L435.1>.

446 DALTON, L.A., BOSAK, T., MACDONALD, F.A., LAHR, D.J.G., AND PRUSS, S.B., 2013,
447 Preservational and morphological variability of assemblages of agglutinated
448 eukaryotes in Cryogenian cap carbonates of northern Namibia: *Palaios*, v. 28, p.
449 67–79, doi: 10.2110/palo.2012.p12-084r.
450 <http://palaios.sepmonline.org/cgi/doi/10.2110/palo.2012.p12-084r>.

451 FERRARI, A.C., AND ROBERTSON, J., 2000, Interpretation of Raman spectra of disordered
452 and amorphous carbon: *Physical Review B*, v. 61, n. 20, p. 14095 – 14097, doi:
453 10.1103/PhysRevB.61.14095.
454 <http://link.aps.org/doi/10.1103/PhysRevB.61.14095>.

455 FLORENZANO, G., SILI, C., PELOSI, E., AND VINCENZINI, M., 1985, *Cyanospira rippkae* and
456 *Cyanospira capsulata* (gen. nov. and spp. nov.): new filamentous heterocystous
457 cyanobacteria from Magadi lake (Kenya): *Archives of Microbiology*, v. 140, p.
458 301–306, doi: 10.3109/00206098409072832.

459 HOFFMAN, P.F., KAUFMAN, A.J., AND HALVERSON, G.P., 1998, Comings and goings of
460 global glaciations on a Neoproterozoic tropical platform in Namibia: *GSA Today*,
461 v. 8, p. 1–9, doi: 10.1130/GSAT01707GW.1.

462 KASEMANN, S.A., HAWKESWORTH, C.J., PRAVE, A.R., FALICK, A.E., AND PEARSON, P.N.,
463 2005, Boron and calcium isotope composition in Neoproterozoic carbonate rocks
464 from Namibia: evidence for extreme environmental change: *Earth and Planetary
465 Science Letters*, v. 231, p. 73–86, doi: 10.1016/j.epsl.2004.12.006.

466 KNOLL, A.H., 1992, Vendian microfossils in metasedimentary cherts of the Scotia Group,
467 Prins Karls Forland, Svalbard: *Palaeontology*, v. 35, p. 751–774.

468 KNOLL, A.H., AND OHTA, Y., 1988, Microfossils in metasediments from Prins Karls
469 Forland, western Svalbard: *Polar Research*, v. 6, p. 59–67.

470 KOBLUK, D.R., AND RISK, M.J., 1977, Algal borings and framboidal pyrite in Upper
471 Ordovician brachiopods: *Lethaia*, v. 10, p. 135–143, doi: 10.1111/j.1502-
472 3931.1977.tb00602.x. <http://dx.doi.org/10.1111/j.1502-3931.1977.tb00602.x>.

473 KOMÁREK, J., AND ZAPOMĚLOVÁ, E., 2007, Planktic morphospecies of the cyanobacterial
474 genus *Anabaena* = subg. *Dolichospermum* - 1. part: coiled types: *Fottea*, v. 7, p.
475 1–31, doi: 10.5507/fot.2007.001.

476 LIU, Y., AND PELTIER, W.R., 2010, A carbon cycle coupled climate model of
477 Neoproterozoic glaciation: influence of continental configuration on the formation
478 of a “soft snowball”: *Journal of Geophysical Research Atmospheres*, v. 115, doi:
479 10.1029/2009JD013082.

480 MADONALD, F.A., MCCLELLAND, W.C., SCHRAG, D.P., AND MACDONALD, W.P., 2009,
481 Neoproterozoic glaciation on a carbonate platform margin in Arctic Alaska and

482 the origin of the North Slope subterranean: Geological Society of America Bulletin ,
483 v. 121, p. 448–473, doi: 10.1130/B26401.1.

484 MANKIEWICZ, C., 1992, *Obruchevella* and other microfossils in the Burgess Shale:
485 preservation and affinity: Journal of Paleontology, v. 66, p. 717–729, doi:
486 10.1017/S0022336000020758.

487 MARGHERI, M.C., PICCARDI, R., VENTURA, S., VITI, C., AND GIOVANNETTI, L., 2003,
488 Genotypic diversity of oscillatoriacean strains belonging to the genera
489 *Geitlerinema* and *Spirulina* determined by 16S rDNA restriction analysis: Current
490 Microbiology, v. 46, p. 359–364, doi: 10.1007/s00284-002-3869-4.

491 MIKHAILYUK, T., HOLZINGER, A., MASSALSKI, A., AND KARSTEN, U., 2014, Morphology
492 and ultrastructure of *Interfilum* and *Klebsormidium* (Klebsormidiales,
493 Streptophyta) with special reference to cell division and thallus formation:
494 European Journal of Phycology, v. 49, p. 395–412, doi:
495 10.1080/09670262.2014.949308.
496 <http://www.tandfonline.com/doi/full/10.1080/09670262.2014.949308>.

497 MOORE, K.R., BOSAK, T., MACDONALD, F.A., LAHR, D.J.G., NEWMAN, S., SETTENS, C.,
498 AND PRUSS, S.B., 2017, Biologically agglutinated eukaryotic microfossil from
499 Cryogenian cap carbonates: Geobiology, v. 15, p. 499-515, doi:
500 10.1111/gbi.12225. <http://doi.wiley.com/10.1111/gbi.12225>.

501 OEHLER, J.H., AND LOGAN, R.G., 1977, Microfossils, cherts, and associated mineralization
502 in the Proterozoic McArthur (H.Y.C) lead-zinc-silver deposit: Economic
503 Geology, v. 72, p. 1393–1409, doi: 10.2113/gsecongeo.72.8.1393.

504 POULÍČKOVÁ, A., ŽIŽKA, Z., HAŠLER, P., AND BENADA, O., 2007, Zygnematalean
505 zygosporae: morphological features and use in species identification: *Folia*
506 *Microbiologica*, v. 52, p. 135–145, doi: 10.1007/BF02932152.

507 RIEDMAN, L.A., PORTER, S.M., HALVERSON, G.P., HURTGEN, M.T., AND JUNIUM, C.K.,
508 2014, Organic-walled microfossil assemblages from glacial and interglacial
509 Neoproterozoic units of Australia and Svalbard: *Geology*, v. 42, p. 1011–1014,
510 doi: 10.1130/G35901.1.

511 ROONEY, A.D., STRAUSS, J. V., BRANDON, A.D., AND MACDONALD, F.A., 2015, A
512 Cryogenian chronology: two long-lasting synchronous Neoproterozoic
513 glaciations: *Geology*, v. 43, p. 459–462, doi: 10.1130/G36511.1.

514 SALMAN, V., BAILEY, J. V., AND TESKE, A., 2013, Phylogenetic and morphologic
515 complexity of giant sulphur bacteria: *Antonie van Leeuwenhoek, International*
516 *Journal of General and Molecular Microbiology*, v. 104, p. 169–186, doi:
517 10.1007/s10482-013-9952-y.

518 SERGEEZ, V.N., AND SCHOPF, J.W., 2010, Taxonomy, paleoecology and biostratigraphy of
519 the late Neoproterozoic Chichkan microbiota of south Kazakhstan: the marine
520 biosphere on the eve of metazoan radiation: *Journal of Paleontology*, v. 84, p.
521 363–401, doi: doi.org/10.1666/09-133.1.

522 SILI, C., MASCALCHI, C., AND VENTURA, S., 2011, Evolutionary differentiation of the
523 cyanobacterial genera *Cyanospira* Florenzano, Sili, Pelosi et Vincenzini and
524 *Anabaenopsis* (Woloszyńska) Miller in response to extreme life conditions:
525 *Fottea*, v. 11, p. 107–117, doi: 10.5507/fot.2011.011.

526 SOROKIN, D.Y., AND CHERNYH, N.A., 2017, *Desulfonatronospira sulfatiphila* sp. nov., and
527 *Desulfitispora elongata* sp. nov., two novel haloalkaliphilic sulfidogenic bacteria
528 from soda lakes: International Journal of Systematic and Evolutionary
529 Microbiology, v. 67, p. 396–401, doi: 10.1099/ijsem.0.001640.
530 <http://www.microbiologyresearch.org/content/journal/ijsem/10.1099/ijsem.0.0016>
531 40.

532 STEINER, M., AND REITNER, J., 2001, Evidence of organic structures in Ediacara-type
533 fossils and associated microbial mats: Geology, v. 29, p. 1119–1122, doi:
534 10.1130/0091-7613(2001)029<1119:EOOSIE>2.0.CO;2.

535 STRAUSS, J.V., MCCLELLAND, W.C., AND MACDONALD, F.A., in press. Pre-Mississippian
536 stratigraphy and provenance of the North Slope subterranean of Arctic Alaska I:
537 Platformal rocks of the northeastern Brooks Range and their significance in
538 circum-Arctic evolution, Geological Society of America Special Papers.

539 TEE, W., DYALL-SMITH, M., WOODS, W., AND EISEN, D., 1996, Probable new species of
540 *Desulfovibrio* isolated from a pyogenic liver abscess: Journal of Clinical
541 Microbiology, v. 34, p. 1760–1764.
542 <http://www.pubmedcentral.nih.gov/articlerender.fcgi?artid=229109&tool=pmcent>
543 [rez&rendertype=abstract](http://www.pubmedcentral.nih.gov/articlerender.fcgi?artid=229109&tool=pmcent).

544 TOMASELLI, L., 1997, *Spirulina Platensis Arthrospira*: Physiology, Cell-Biology And
545 Biotechnology (A. Vonshak, Ed.): Taylor & Francis Ltd., London, 1-15 p.

546 TOMASELLI, L., BOLDRINI, G., AND MARGHERI, M.C., 1997, Physiological behaviour of
547 *Arthrospira (Spirulina) maxima* during acclimation to changes in irradiance:
548 Journal of Applied Phycology, v. 9, p. 37–43, doi: 10.1023/A:1007956210329.

549 TZIPERMAN, E., ABBOT, D.S., ASHKENAZY, Y., GILDOR, H., POLLARD, D., SCHOOF, C.G.,
550 AND SCHRAG, D.P., 2012, Continental constriction and oceanic ice-cover
551 thickness in a Snowball-Earth scenario: *Journal of Geophysical Research: Oceans*,
552 v. 117, C05016, doi: 10.1029/2011JC007730.

553 WACEY, D., MCLOUGHLIN, N., KILBURN, M.R., SAUNDERS, M., CLIFF, J.B., KONG, C.,
554 BARLEY, M.E., AND BRASIER, M.D., 2013, Nanoscale analysis of pyritized
555 microfossils reveals differential heterotrophic consumption in the ~1.9-Ga
556 Gunflint chert: *Proceedings of the National Academy of Sciences of the United*
557 *States of America*, v. 110, p. 8020–8024, doi: 10.1073/pnas.1221965110.
558 [http://www.pubmedcentral.nih.gov/articlerender.fcgi?artid=3657779&tool=pmce](http://www.pubmedcentral.nih.gov/articlerender.fcgi?artid=3657779&tool=pmcentrez&rendertype=abstract)
559 [ntrez&rendertype=abstract](http://www.pubmedcentral.nih.gov/articlerender.fcgi?artid=3657779&tool=pmcentrez&rendertype=abstract).

560 WONGSAWAD, P., AND PEERAPORNPISAL, Y., 2015, Morphological and molecular profiling
561 of *Spirogyra* from northeastern and northern Thailand using inter simple sequence
562 repeat (ISSR) markers: *Saudi Journal of Biological Sciences*, v. 22, p. 382–389,
563 doi: 10.1016/j.sjbs.2014.10.004. <http://dx.doi.org/10.1016/j.sjbs.2014.10.004>.

564 XIAO, S., 2004, New multicellular algal fossils and acritarchs in Doushantuo chert nodules
565 (Neoproterozoic; Yangtze Gorges; south China): *Journal of Paleontology*, v. 78,
566 p. 393–401, doi: 10.1666/0022-3360(2004)078<0393:NMAFAA>2.0.CO;2.

567 ZAARUR, S., WANG, D.T., ONO, S., AND BOSAK, T., 2017, Influence of phosphorus and cell
568 geometry on the fractionation of sulfur isotopes by several species of
569 *Desulfovibrio* during microbial sulfate reduction: *Frontiers in Microbiology*, v. 8,
570 doi: 10.3389/fmicb.2017.00890.

571 ZHANG, Y., YIN, L., XIAO, S., AND KNOLL, A.H., 1998, Permineralized fossils from the
572 terminal Proterozoic Doushantuo Formation, south China: Journal of
573 Paleontology, v. 72, p. 1–52.

574

575 FIGURE CAPTIONS

576

577 FIG. 1.—Stratigraphic column of the Sadlerochit and Kikiktat Mountains and the Fourth
578 Range of Artic Alaska (Strauss et al., accepted; Macdonald et al., 2009 and
579 references therein). Samples (labeled in green as F609) come from the base of the
580 Ikiakpuk formation in the Fourth Range.

581

582 FIG. 2.—SEM images of dominant coil morphologies. Morphologies include tightly
583 coiled helices with fine crystalline granular texture (A, B, C, D), loosely coiled
584 helices with fine crystalline granular texture (E), loosely coiled helices with some
585 framboids embedded within the fine crystalline granular texture, and broken coils
586 showing solid cross sections of the strands comprising the coils (G, H).

587

588 FIG. 3.—SEM images of other morphologies. Strands are curved with uniform thickness
589 throughout the specimen and comprised of framboids (A, B), straight with
590 framboids and some areas of fine crystalline granular texture (C, D), or curved
591 and comprised of framboids that taper toward a narrow point (E, F).

592

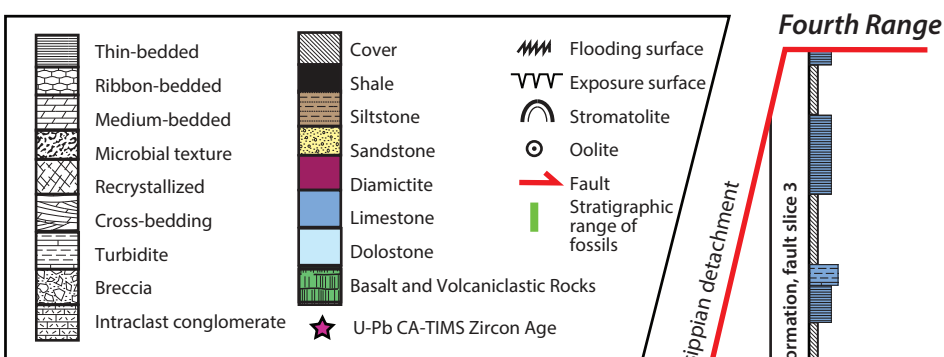
593 FIG. 4.—EDS chemical map of a representative coil. Chemical maps show the
594 compositional distribution of all elements present (A, B) and demonstrate a clear
595 dominance of Fe (C) and S (D) covering the structure.

596

597 FIG. 5.—Raman spectrum of a representative coil demonstrating dominant peaks at ~1348
598 cm^{-1} and ~1609 cm^{-1} , consistent with D-band and G-band Raman shift indicative
599 of organic carbon (e.g., Ferrari and Robertson, 2000; McNeil et al., 2015).

600

601 FIG. 6.—Petrographic thin section of a representative limestone of the Ikiakpuk
602 formation showing dark circles (outlined in dotted lines). These circles are rarely
603 observed in thin section due to the surrounding dark micrite, and show cross-
604 sections through the solid pyritized strands.



Sadlerochit Mountains

